Anomalous Plasma Transport in the Stochastic Magnetic Field

Kubota, Tetsuyuki
Interdisciplinary Graduate School of Engineering Sciences, Kyushu University

Yagi, Masatoshi
Research Institute for Applied Mechanics, Kyushu University

Ito, Sanae-I.
Research Institute for Applied Mechanics, Kyushu University

https://doi.org/10.5109/6786333

出版情報：Reports of Research Institute for Applied Mechanics. 41 (112), pp.1-22, 1995-09. 九州大学応用力学研究所

Reports of Research Institute for Applied Mechanics
Vol. XXXXI No. 112, 1995

Anomalous Plasma Transport in the Stochastic Magnetic Field

By Tetsuyuki KUBOTA+, Masatoshi YAGI* and Sanae-I. ITOH*

The anomalous transport of a high temperature plasma in the region of stochastic magnetic field is studied. Toroidal plasmas, such as tokamak's, are considered. Using the kinetic equation for plasma particles in the stochastic magnetic field, the plasma transport matrix in the stochastic region is formulated. A quasilinear approximation for the diffusivity of the magnetic field line D_M is used. The shifted Maxwellian which includes the mean velocity and the self-consistent electric potential is assumed. By use of this transport matrix the radial electric field formation, which is generated by ambipolar condition, and the associated temperature distribution in the stochastic region is obtained. The temperature distribution in the stochastic region becomes flat because of the rapid temperature diffusion. The radial electric field is formed in the stochastic region and its magnitude is found to depend on the value of D_M, and on the conditions of the heat fluxes and temperature gradients of electrons and ions in the non-stochastic region.

Contents

Key words: anomalous transport, tokamak, plasma, stochastic magnetic field, radial electric field, sawtooth

I. Introduction

The problem of plasma transport in the presence of magnetic fields which are

+ Interdisciplinary Graduate School of Engineering Sciences, Kyushu University
* Research Institute for Applied Mechanics, Kyushu University

assumed to be stochastic has received considerable attentions because of its importance in providing an explanation of the anomalous plasma transport in tokamaks[1]. The research has been made to provide an explanation of the electron heat transport due to parallel thermal conductivity in the collisional and collisionless limits for the case of destroyed magnetic surfaces[2)3)]. The importance of this for anomalous transport lies in the rapid rate at which heat flows along a magnetic field line. The heat is carried by particles at their thermal speed without collision and thus principal by electrons.

Other than the thermal conductivity[4)~7)], a little work has focused on the electron viscosity[8)], i. e., hyper resistivity[9)]. The calculation of the elements in the form of transport matrix has rarely been done.

Ergodization of the magnetic field structure occurs when the magnetic islands overlap each other. In a tokamak plasma, a stochastic region near the mode rational surface, for example $q=1$, 2, $\cdots$, surface, has been predicted to appear due to the nonlinear interaction in three dimensions of MHD tearing modes with different pitch[10)11)]. The behavior of magnetic field can be described by the Hamiltonian formalism and has been analyzed[12)13)]. The primary islands appear to take small perturbation to the Hamiltonian. And if perturbation is large enough, then the higher order islands appear. Second order islands grow exponentially with respect to the main island size, and primary islands overlap with it, so that the stochastic magnetic field is produced.

The recent theoretical analysis has shown that the global stochasticity sets in when the MHD mode grows and the perturbation reaches to the threshold value[14)]. The process is triggered and is enhanced by the current diffusivity (i. e., electron viscosity), whose magnitude is anomalously increased by the magnetic stochasticity itself. As is well known, the global mode stability is strongly dictated by the transport coefficients near the mode rational surface[15)~17)], the relevant transport coefficients for the mode are to be obtained.

From the view point of the plasma confinement, stochastic magnetic field has received the strong attention. However, we do not have enough understanding for the plasma transport in the stochastic magnetic field region.

Furthermore, the radial electric field has received the strong attention in connection with the plasma transport and enhanced confinement[18)]. What has been found in experiments is the existence of not only the edge electric field in the H-mode discharges, but also the internal electric field structure in another enhanced mode[19)]. The reason why such radial electric field exists is not yet clear. The contribution from the diffusion in the stochastic magnetic field is a candidate, since the particle diffusion is intrinsically bipolar, which may cause the radial electric field. The formulation of the transport matrix in the presence of the stochastic magnetic field will give a base to understand the transport process as well as the global mode stability of toroidal plasmas.

In this paper, we formulate the transport matrix for a cylindrical plasma in a stochastic magnetic field, where quasilinear approximation is used for the amplitude of the magnetostatic perturbation in a collisionless limit. The radial gradient of parallel flow is included as a thermodynamical force. The elements including the off-diagonal terms are derived. As an application, a formation of static electric field and the associated temperature distribution are analyzed. Topic will be focused on the ambipolar electric field due to the particle diffusion, and the thermal conduction, and on the parallel thermoelectric field caused by the thermal conduction.

The organization of this paper is as follows. In Sec. II we survey the dynamics of the magnetic field line which is used to describe the magnetic stochasticity, theoretical models of the anomalous particles diffusion and electron heat transport in the stochastic magnetic field lines. The experimental result of the temperature disruption in tokamak plasma is briefly discussed. In Sec. III, the 3×3 transport matrix in a stochastic magnetic field for each species is derived. Using the obtained coefficients in Sec. III, the formation of electric field and temperature distribution are examined in Sec. IV. Summary and discussions will be given in Sec. V.

II. Review

In this section we survey the magnetic stochasticity and the anomalous plasma transport in the stochastic magnetic field. At first we review the dynamics of the magnetic field line and occurrence of the magnetic stochasticity. Secondly the theoretical models of the anomalous plasma transport are reviewed. Thirdly the experimental results of the disruptive phenomena are reviewed.

The magnetic topology in a plasmas under toroidal confinements is described as nested magnetic surfaces. Their existence is easily demonstrated when the magnetic field possesses toroidal symmetry; an asymptotic calculation indicates their presence under a much more general set of conditions. On the other hand, it is well known that lack of symmetry, which is made from MHD instability, in the magnet windings can lead to the appearance of magnetic islands and stochastic magnetic field lines.

A Hamiltonian formalism is used to describe the behavior of magnetic field line[14]. In the tokamak configuration shown in Fig. (1), the toroidal coordinate ϕ plays the role of times in the usual dynamic system. When the equilibrium magnetic field forms a closed flux surface, the periodic motion of the unperturbed field is conveniently described in terms of the action angle variables J and θ. The action J labels the flux surface, and the change of the angle θ of the unperturbed field line is given by

$$\frac{d\theta}{d\phi} = -\frac{dH_0(J)}{dJ} = \iota(J), \tag{2.1}$$

where in the case of a circular cross-section, $J = r^2/2$ and $\iota = RB_r/rB_\phi$.

In the presence of a perturbed field, the Hamiltonian of the field line takes the

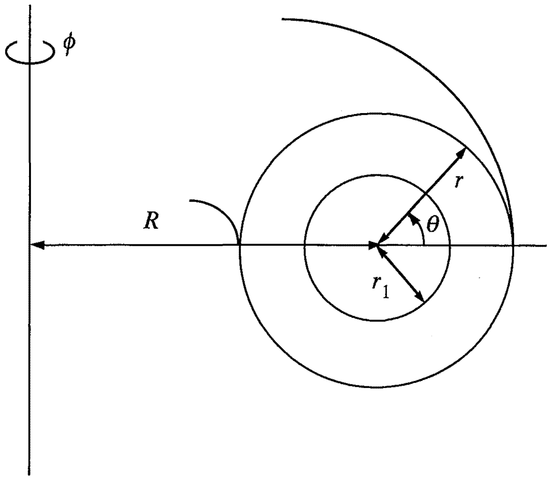

Fig. 1 The model tokamak geometry. R, r, ϕ and θ are the major radius, minor radius, toroidal coordinate and poroidal coordinate, respectively. r_1 is the $m/n=1/1$ surface.

form as

$$H(J,\ \theta,\ \phi) = H_0(J) + \sum A_{mnk}(\sqrt{2J}/R_0)^{|k|} e^{i(m+k)\theta - in\phi}, \tag{2.2}$$

where the summation over k is the expansion of the toroidal correction, and m and n are the poloidal and toroidal mode numbers of the perturbation. The amplitude of the perturbation A_{mnk} is related to the radial magnetic field B_r as

$$A_{mnk} \simeq \frac{rR_0 B_{rmn}}{i(n+k)B_{\phi 0}}. \tag{2.3}$$

We shall assume that the primary island amplitude is determined by the lowest order perturbation term $m = n = 1$. Equation (2. 2) is transformed to new variations in a rotating coordinate system, $\hat{J}$ and $\hat{\theta}$, and is expanded around the resonant magnetic surface J_0, where $\iota(J_0) = 1$,

$$\begin{aligned} \hat{\theta} &= \theta - \phi, \\ \Delta J &= J - J_0,\ (\hat{J} = J) \end{aligned} \tag{2.4}$$

giving the Hamiltonian for the perturbation as

$$H(\hat{J},\ \hat{\theta},\ \phi) \simeq -\left.\frac{d\iota}{dJ}\right|_{J=J_0} \frac{(\Delta J)^2}{2} + A_{11}\cos(\hat{\theta})$$
$$+ \sum A_{mnk}(r_1/R_0)^{|k|} e^{i(m+k)\theta - i(m+k-n)\phi}, \tag{2.5}$$

where the higher order terms are neglected, Eq. (2. 5) is evaluated the perturbation at J_0 and is added the ± 1 terms.

Averaging over the fast variable ϕ, the pendulum Hamiltonian characterizing the m/n=1/1 island is obtained as

$$K_0 = G(\Delta J)^2/2 + F\cos(\hat{\theta}), \tag{2.6}$$

where $F = A_{11}$ and $G = -\frac{d\iota}{dJ}$. Substituting Eq. (2. 3) for A_{11} and using a parabolic approximation for ι, F and G are written in terms of the field as

$$F = r_1 R_0 \frac{B_r}{B_\phi} \equiv r_1{}^2 \tilde{B}_n, \tag{2.7}$$

$$G = \frac{2(\iota(0)-1)}{r_1{}^2} \equiv 2\frac{s}{r_1{}^2}, \tag{2.8}$$

where $\tilde{B}_n$ is the normalized perturbation field and $s = \iota(0)-1$ is the normalized shear. The amplitude of the island and the frequency at the fixed point are given by

$$\Delta J_M = 2(F/G)^{1/2} = (8\tilde{B}_n/s)^{1/2} J_0, \tag{2.9}$$

$$\omega_0 = (FG)^{1/2} = (2\tilde{B}_n s)^{1/2}. \tag{2.10}$$

The first order magnetic island is shown by Fig. (2).

If the perturbation amplitude is large enough the second order islands appear. A lot of second order islands are formed like a chain near the separatrix of the first order island. The second order islands overlap each other with enlargement of the perturbation amplitude. Magnetic field lines are become stochastic at the overlapping region. Therefore the thickness of the stochastic region is estimated by the condition of the second order overlapping. To obtain the thickness of the stochastic region, the variables in the pendulum Hamiltonian is transformed by the new action-angle variables, to exhibit the second order island[20)21)]. The overlap for two second order island chains leads to a stochastic region with

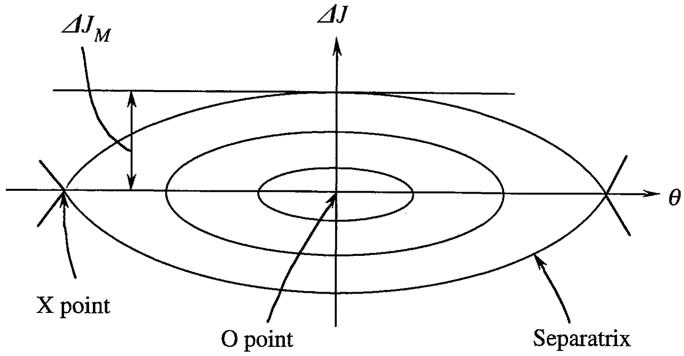

Fig. 2 The primary islands structure in the phase space($\Delta J - \theta$). ΔJ_M is the width of the primary island. X point is the reconnection point. The separatrix is the boundary line of the primary islands.

$$\delta J_S = 2\left(\frac{F}{G}\right)^{1/2}\frac{4\pi}{(FG)^{3/2}}\exp\left(-\frac{\pi}{2(FG)^{1/2}}\right), \tag{2.11}$$

δJ_S being the half-thickness of the stochastic region, which is approximately equal inside and outside the separatrix. The edges of the regular region outside and inside the separatrix are then calculated from

$$\varDelta J_T = \varDelta J_M \pm \delta J_S. \tag{2.12}$$

This result can also be easily transformed to physical space, using

$$r = r_1(1-\varDelta J_T/J_0)^{1/2}, \tag{2.13}$$

and $\varDelta r_T = r - r_1$. The result of Eq. (2.13) is plotted in Fig. (3). The stochastic region is increased rapidly with the perturbation amplitude.

The plasma transport in the stochastic magnetic field region is much different from the nested magnetic field line by the turbulence of the magnetic field line. The trapped particles are turbulenced with the turbulence of the magnetic field line[22]. This particle turbulence is represented by the quasilinear formalism. The mean magnetic field B and perturbed magnetic field B_x which is perpendicular to the mean magnetic field are assumed, where the z-axis is the direction of mean magnetic field line and x-axis is the perturbation direction (Fig. (4)). It is assumed that the plasma particles move with constant velocity v_z along the magnetic field line. The plasma particle diffusivity D_P along x-axis is described as

$$D_P = v_z D_M, \tag{2.14}$$

where

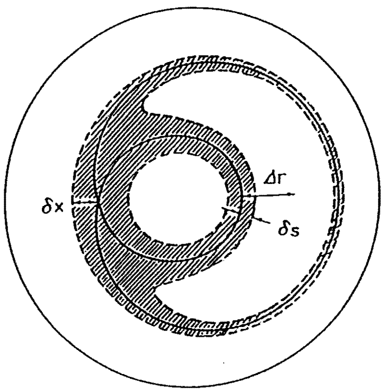

Fig. 3 Magnetic island and stochastic region. Δr δ_s and δ_x indicate the width of the main magnetic island, the thickness of the stochastic layer near the O-point and the thickness of the stochastic layer near the X-point, respectively. (Cited from Fig. 1(b) in Ref. 14)

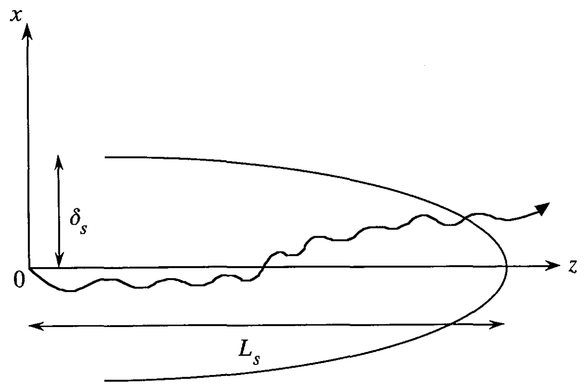

Fig. 4 The relation between the correlation length and the particle diffusion. In the elliptic line region, the particle correlates with the turbulence at the origin. The correlation decays when the particle moves L_s away. (Cited from Fig. 5 in Ref. 22)

$$D_M = \int_{-\infty}^{\infty} ds \langle b(\boldsymbol{r}(s),\ s) b(\boldsymbol{r}(0),\ 0) \rangle, \tag{2.15}$$

$b(\boldsymbol{r},\ s) = B_x(\boldsymbol{r},\ s)/B,$

and D_M is the magnetic field line diffusivity.

The correlation between the $b(\boldsymbol{r}(s),\ s)$ and $b(\boldsymbol{r}(0),\ 0)$ decays while the particle moves a distance of s away along the braided magnetic field line (Fig. (4)). Although the particle does not move enough x direction and the particle exists in the same magnetic surface, the turbulence B_x loses the correlation with initial condition while the particle moves L_S away with the evolution. Therefore the integration length is from 0 to L_S at the Eq. (2. 15) and the magnetic field line diffusivity is obtained as

$$D_M = b^2 L_S. \tag{2.16}$$

D_M is proportional to the square of the turbulent magnetic field. Therefore the plasma particle diffusion to the perpendicular direction in the stochastic magnetic field represented by the quasilinear formalism.

The electron heat transport in the magnetic stochasticity is considered[3]. This transport is caused by the parallel thermal conductivity in a tokamak with destroyed magnetic surfaces. To treat the electron heat transport, the geometric characteristics of the stochastic magnetic field is important. The magnetic configuration in cylindrical geometry is used as

$$\vec{B} = B_z \vec{z} + B_\theta(r) \vec{\theta} + \delta \vec{B}, \tag{2.17}$$

where $\delta \vec{B}$ is the perturbed term as

$$\delta\vec{B} = \sum_{m,n} \vec{b}_{mn}(r)\exp[i(m\theta - nz/R]. \tag{2.18}$$

In order to model toroidal periodicity, it is assumed that the system is periodic in the z direction with period $2\pi R$[24].

Considering a small circle of radius l_0 in the plane z=const, the magnetic field lines in this plane can be mapped by solving the equation

$$\frac{dr}{dz} = \frac{B_r}{B_z} \text{ and } r\frac{d\theta}{dz} = \frac{B_\theta}{B_z}. \tag{2.19}$$

This magnetic mapping is area preserving, as a consequence of the equation

$$\nabla \cdot \vec{B} = 0. \tag{2.20}$$

There will be two different stages of evolution of this area. First, it will move as a whole, and it will deform its shape stretching in one direction and contracting in the other. This behavior is called stochastic instability of trajectories. This process can be described analytically for continuous mapping by the equation as

$$l(z) = l_0\exp(z/L_c), \tag{2.21}$$

where L_c is the correlation length for the simple mapping corresponding to islands of fixed m with different n[25]. The width δ of the area exponentially decreases in order to conserve the total area, i. e.,

$$\delta(z) = l_0\exp(-z/L_c). \tag{2.22}$$

All processes of mapping are strictly reversible, but because the width of the area becomes extraordinarily small, any small spreading due to motion perpendicular to the field line can be of great importance.

The evolution of the area looks very complicated, as depicted in Fig. (5). It

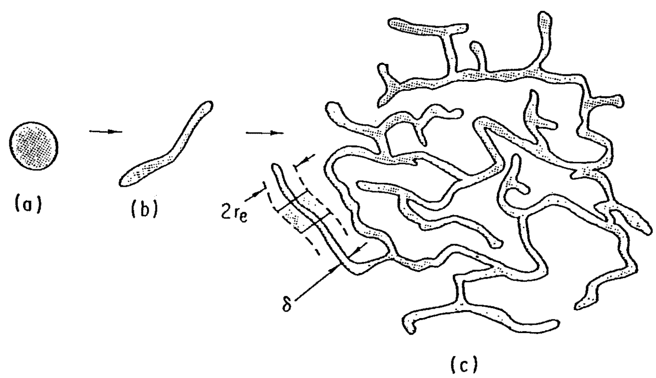

Fig. 5 The evolution of area mapping. Moving the small circle along the trajectory, this small circle is mapped into a complicated thin region and the width δ of the area exponentially decreases in order to conserve the total area. (Cited from Fig. 1 in Ref. 3)

can be shown that the average squared radial displacement of the area can be described by a diffusion formula

$$\langle(\Delta r)^2\rangle = 2LD_{st}, \tag{2.23}$$

where L is the distance in the z direction, which is much longer than the correlation length for the area and D_{st} is the diffusion coefficient of the stochastic magnetic field line[26].

It is assumed that guiding-center trajectories coincide with the field lines and just one "particle" is spread over some initial area of the dimension r_e, instead of considering many discrete particles. It moves before colliding a distance $\lambda = \nu\tau$ along the trajectory, mapping into a complicated thin region of the kind drawn in Fig. (5), with the width

$$\delta \simeq r_e \exp(-\lambda/L_c) \tag{2.24}$$

The average squared displacement of its elements in a radial direction is equal to

$$\langle(\Delta r)^2\rangle = 2D_{st}\lambda. \tag{2.25}$$

For the case of $r_e \gg \delta(\lambda)$ which is collisionless case, each of these new elements will evolve on second step almost independently from its previous history. Therefore the spreading of our area in the radial direction is similar to a random walk and the diffusion coefficient is given by

$$\chi_r = \langle(\Delta r)^2\rangle/2t, \tag{2.26}$$

where $\langle(\Delta r)^2\rangle$ is the mean square of the radial displacement of electrons during the time interval t. For the collisionless case the guiding-center trajectories coincide with the field line. The thermal diffusion coefficient in the area is given by

$$\chi_r = \langle(\Delta r)^2\rangle/2\tau = D_{st}v, \tag{2.27}$$

where τ and v are the collision frequency and particle velocity along the trajectory, respectively. This diffusion time is smaller than the classical diffusion time.

For the collisional case any substantial spreading of the area in the radial direction due to the mapping will take place after the particle has collided many times. There will be two competing processes which are the stochastic instability and the perpendicular classical diffusion. Considering the balance of two processes, the correlation length for the areas, which is cut into small pieces δ, is written as

$$L_{c\delta} = L_c \ln[(r/mL_c)(\chi_{/\!/}/\chi_\perp)^{1/2}], \tag{2.28}$$

with the corresponding time for parallel diffusion $t_\delta \sim L_{c\delta}{}^2/\chi_{/\!/}$, where $\chi_{/\!/}$ and $\chi_\perp$ are the parallel and perpendicular classical diffusion conductivities, respectively. Thus, t_δ is the time during which a particle may be thought of as orbiting along a single field line before diffusing to a new field line whose trajectory is no longer correlated with the original one. This complicated continuous evolution can be considered simply as a random walk with the step size

$$\langle(\Delta r)^2\rangle = D_{st}L_{c\delta}. \tag{2.29}$$

Therefore the thermal diffusion coefficient is given by

$$\chi_r = D_{st}\chi_{/\!/}/L_{c\delta}, \tag{2.30}$$

In the previous argument, it is obtained that the electron heat transport in the magnetic stochasticity is much larger than the classical diffusion. It is known that the enhanced heat transport in the stochastic magnetic field may give rise to the temperature disruption in tokamak plasma.

Disruptive phenomenon is a common feature of ohmic and additionally heated plasma in the majority of tokamaks. Disruptive phenomena in tokamak, such as sawtooth oscillation and major disruption, are characterized by initial slow growth of a magnetic perturbation followed by a rapid mode growth and a fast temperature crash. In the ST tokamak, fluctuations in X-ray intensity were observed which shown a characteristic sawtooth behavior (Fig. (6))[26]. The soft X-ray intensity shows the electron density and temperature, and the X-ray

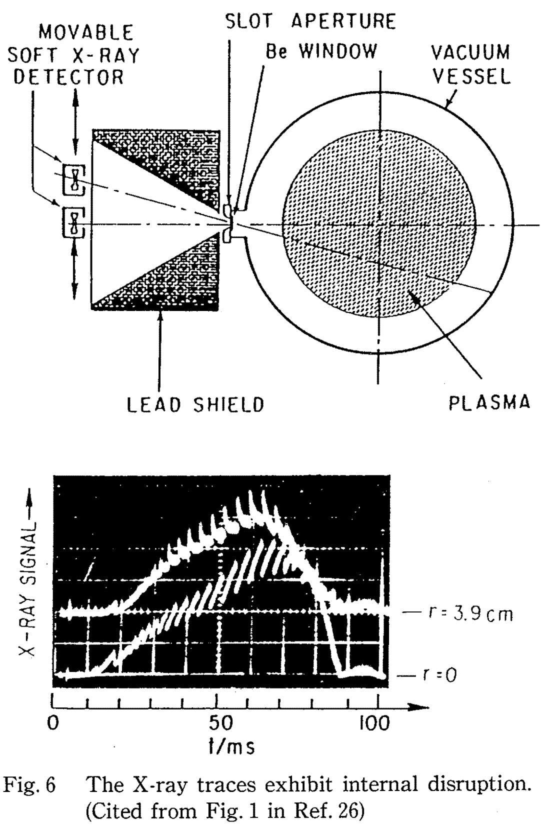

Fig. 6 The X-ray traces exhibit internal disruption. (Cited from Fig. 1 in Ref. 26)

fluctuations were caused by a fluctuation in either of these quantities, but predominantly temperature fluctuations. Therefore sawtooth oscillation indicates the temperature sawtooth oscillation.

In a theoretical model of the sawtooth oscillation proposed by Kadomtsev[5], the temperature at the plasma centre increases slowly during the ramp phase, because of Ohmic heating. The resulting increase in current density takes the safety factor, q, below unity in the central region, leading to an $m=1$ instability which is observed as a precursor to the rapid sawtooth disruption phase. It is hypothesized that the disruption is the result of a growing magnetic island at the $q=1$ surface which leads to a rapid reconnection of magnetic field lines. The reconnection is assumed to lead to a stable configuration with $q>1$, simultaneously producing the observed flattening of the temperature and density profiles. This cycle is then repeated (Fig. (7)).

On the other hand a detailed sawtooth activity was observed in ohmically heated JET plasma by the measurements of soft X-ray and electron cyclotron emission (ECE)[27]. This study was revealed a variety of features, several of which appear to be inconsistent with the magnetic reconnection (Kadomtsev)

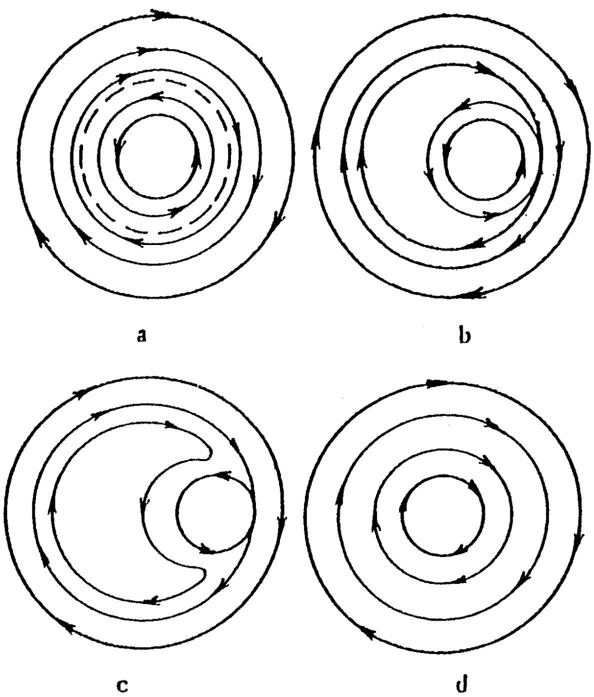

Fig. 7 a) The magnetic surfaces in initial state. b, c) During reconnection due to the finite conductivity. d) After reconnection. (Cited from Fig. 1 in Ref. 5)

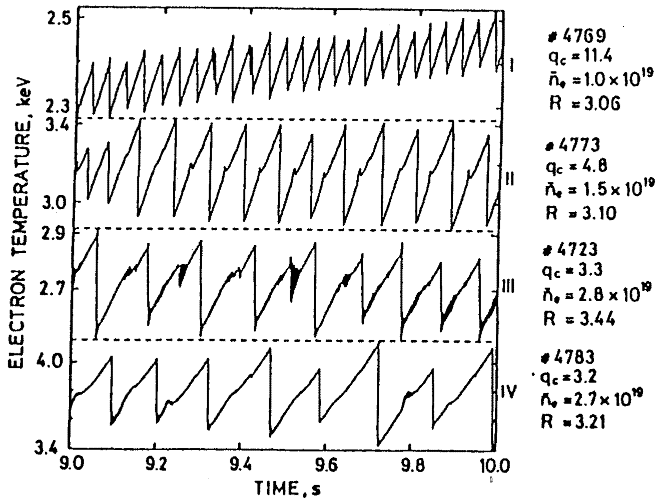

Fig. 8 The sawtooth oscillation for widely varying plasma parameters. The toroidal magnetic field was 3.4 T in each case and the plasma current was (i) 1MA (ii) 2 MA (iii) 3MA (iv) 4MA. (Cited from Fig. 7 in Ref. 27)

model of the internal disruption[5] and its derivatives[28][29]. Figure (8) shows the temperature sawtooth oscillation and figure (9) shows the details of the temperature sawtooth disruption from JET discharges with widely varying plasma parameters. The sawtooth disruption time observed in JET are very short, typically about $100\mu s$, but sometimes as short as $50\mu s$ (Fig. (9)). This is comparable with the disruption time observed on much smaller tokamak and is significantly shorter than the time predicted theoretically, which is $\sim$10ms. This is 100 times longer than the observed time.

For the explanation of the temperature disruption the magnetic stochasticity model is presented. An alternative picture of the disruptive sawtooth phase can be drawn by using the concept of intrinsic stochasticity driven by the strong interaction or 'overlapping' of island chains with different helicity. A pioneering study, using this concept, described the destruction of magnetic surfaces in a stellarator as due to the interaction of the phenomenon were subsequently carried out, including both external-field perturbation and perturbations arising from unstable modes. As described previously the heat conductivity in the stochastic magnetic region is much larger than that in the non-stochastic region. In the stochastic region, the radial diffusion of the magnetic field lines with diffusivity, D_M, strongly enhances the electron thermal diffusivity

$$\chi_\perp = (3/\sqrt{\pi}) n v_{Te} D_M, \tag{2.29}$$

where n and v_{Te} are density and thermal velocity. This thermal diffusivity is

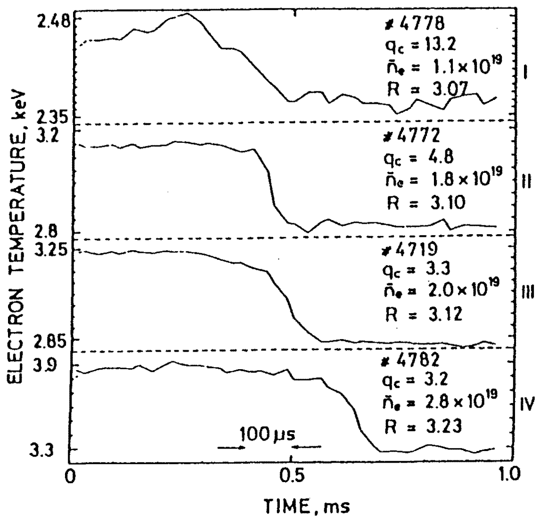

Fig. 9 Sawtooth disruption times for widely varying plasma parameters from the ECE Fabry-Perot diagnostic. The toroidal magnetic field was 3. 4T in each current was (i) 1MA (ii) 2MA (iii) 3MA (iv) 4MA. (Cited from Fig. 6 in Ref. 27)

over the classical collisional values and the electron heat diffusion time scale is $\sim 25\mu s$. This value is consistent with the JET observation. Therefore we may say that the plasma transport in the stochastic magnetic field plays an important role of the plasma confinement.

III. Formulation of Transport Matrix

In this section, we present our theoretical model and formulae of the anomalous particle, momentum and energy fluxes due to magnetostatic turbulence, i. e., magnetic stochasticity. We consider a cylindrical plasma immersed in a strong magnetic field in the z-direction. The poloidal magnetic field is assumed to be small. Even in the presence of the magnetic braiding, the strength of the field is to be represented by the ensemble averaged value. The plasma is inhomogeneous in the radial direction.

We start our analysis with the kinetic equation which has been used to derive the thermal diffusivity and the current diffusivity[14]. We extend the argument in the following. When the gyroradius, ρ, is small compared with the inhomogeneity scale lengths, the kinetic equation for electrons and ions in the presence of magnetic stochasticity can be written,

$$\frac{\partial f}{\partial t}+\mathbf{v}\cdot\nabla f+\frac{q}{m}(\mathbf{E}+\mathbf{v}\times\mathbf{B})\cdot\nabla_{\mathrm{v}}f=\frac{\partial}{\partial x}(|v_{/\!/}|D_M)\frac{\partial f}{\partial x}+C(f),\tag{3.1}$$

where $C(f)$ is a collision operator and

$$D_M=(\delta r)^2/2\pi R_0$$

indicates the diffusivity of the magnetic field line in the presence of stochasticity during which the field lines step a random distance δr in going once around the torus, where R_0 is the major radius. We here restrict to the collisionless limit and the quasilinear value is taken for D_M. We assume that the D_M is uniform within the region of our interest.

To obtain matrix elements we shall take the moments of Eq. (3. 1), specifying the unperturbed velocity distribution function. The plasma is assumed to be in a steady state. Thus the velocity distribution $f_{0\sigma}$ is a function of the energy, $m_\sigma v^2/2+q_\sigma\phi$, where ϕ is the static potential, and canonical momenta in the θ and parallel directions,

$$P_\theta=m_\sigma r(v_\theta+r\Omega_\sigma/2)\ \text{and}\ P_{/\!/}=m_\sigma v_{/\!/},$$

respectively. More specifically, we adopt a local shifted Maximilian distribution as

$$f_{0j}=f_{0\perp j}\cdot f_{0/\!/j},\tag{3.2}$$

$$f_{0/\!/j}=\frac{1}{\sqrt{\pi}}\sqrt{\frac{m_j}{2T_{/\!/j}(x)}}\exp\left[-\frac{m_j(v_{/\!/j}(x)-U_{/\!/j}(x))^2}{2T_{/\!/j}(x)}\right],$$

$$f_{0\perp j}=\frac{1}{\pi}\frac{m_jn_j(x)}{2T_{\perp j}(x)}\exp\left[-\frac{m_jv_{\perp j}(x)^2}{2T_{\perp j}(x)}-\frac{e\phi(x)}{\langle T\rangle}\right],$$

where $j=i,\ e,\ T_{/\!/j}(x)$ and $T_{\perp j}(x)$ are the parallel and perpendicular temperatures, $U_{/\!/j}(x)$ is the mean velocity along the parallel direction, $\phi(x)$ is the self-consistent electric potential, $\langle T\rangle$ is the local averaged temperature to normalize $\phi(x)$, and m_j, n_j are particle mass and density. Here r is expanded around r_0 with respect to gyroradius and a new coordinate x given by

$$x=r-r_0+v_\theta/\Omega_\sigma$$

is used.

Taking the O-th to the second moments of Eq. (3. 1), we obtain

$$m_j\left(\frac{\partial n_j}{\partial t}+\nabla\cdot(n_j\boldsymbol{U}_j)\right)=-\frac{\partial}{\partial x}\Gamma^M_{xj},\tag{3.3}$$

$$\left[m_jn_j\left(\frac{\partial \boldsymbol{U}_j}{\partial t}+\boldsymbol{U}_j\cdot\nabla\boldsymbol{U}_j\right)-\frac{q_j}{c}\Gamma_j\times\boldsymbol{B}+\nabla\cdot p_j\right]=-\frac{\partial}{\partial x}P^M_{xj}$$
$$+[n_jq_j\boldsymbol{E}-\nabla\cdot(P_j-p_jI)],\tag{3.4}$$

$$\frac{\partial}{\partial t}(3p_j)+\nabla\cdot\boldsymbol{Q}_j+2P_j\cdot\nabla\boldsymbol{U}_j=-\frac{\partial}{\partial x}Q^M_{xj}+q_j(\Gamma_j-n_j\boldsymbol{U}_j),\tag{3.5}$$

for each article species. $\Gamma_j=n_jU_j$, represents the particle flux defined by $\int vf_jd^3v$, $n_j=\int f_jd^3v$ is the density,

$$p_j = n_j T_j (\equiv \int m_j (v_{j,l} - U_{j,l})^2 f_j d^3 v)$$

is the pressure, $U_{j,l}$ is the mean velocity, and

$$Q_{j,l} = 3 T_j \Gamma_{j,l} + \sum Q_{j,lmm}$$

is the heat flux, where

$$Q_{j,lmn} = \int m_j (v_{j,l} - U_{j,l})(v_{j,m} - U_{j,m})(v_{j,n} - U_{j,n}) f_j d^3 v$$

is the heat conduction, P_j is the stress tensor and I is the unit tensor. Here the indices l, m, n stand for the three coordinates, r, θ, z, respectively. In this article only $U_{/\!/ j}$ is considered as the mean velocity. Terms Γ^M_{xj}, P^M_{xj} and Q^M_{xj} are the particle, momentum and heat fluxes induced by the magnetic stochasticity where the subscript x stands for the direction which is perpendicular to the mean magnetic field line. They are given by

$$\Gamma^M_{xj} \equiv -\int |v_{/\!/ j}| D_M \frac{\partial f_{0j}}{\partial x} d^3 v_j, \tag{3.6}$$

$$P^M_{xj} \equiv -\int |v_{/\!/ j}| m_j (v_{/\!/ j} - U_{/\!/ j}(x)) D_M \frac{\partial f_{0j}}{\partial x} d^3 v_j, \tag{3.7}$$

$$Q^M_{xj} \equiv -\int |v_{/\!/ j}| \frac{1}{2} m_j (v_{/\!/ j} - U_{/\!/ j}(x))^2 D_M \frac{\partial f_{0j}}{\partial x} d^3 v_j. \tag{3.8}$$

In order to calculate the above fluxes, the integrals of

$$\frac{1}{v_{T/\!/}{}^{m+1}} \int_{-\infty}^{\infty} |v_{/\!/}| (v_{/\!/} - U_{/\!/ j}(x))^m f_{0/\!/} dv_{/\!/}, \tag{3.9}$$

for $m = 0$, 1, 2, 3 and 4 are needed. Performing the integration, we define the thermodynamic forces as

$$X_{1j} = \frac{1}{n_j} \frac{dn_j}{dx} - \frac{1}{2} \frac{1}{T_j} \frac{dT_j}{dx} \pm \frac{e}{\langle T \rangle} \frac{d\phi}{dx}, \tag{3.10}$$

$$X_{2j} = \frac{2}{v_{Tj}} \frac{dU_{/\!/ j}(x)}{dx}, \tag{3.11}$$

$$X_{3j} = \frac{1}{T_j} \frac{dT_j}{dx}, \tag{3.12}$$

where $v_{Tj} \equiv \sqrt{\frac{2T_j}{m_j}}$ is thermal velocity, for $T_{/\!/ j} = T_{\perp j} \equiv T_j$, Introducing normalized quantities given by,

$$\hat{\Gamma}^M_{xj} = \Gamma^M_{xj} / n_j v_{Tj},$$
$$\hat{P}^M_{xj} = P^M_{xj} / m_j n_j v_{Tj},$$
$$\hat{Q}^M_{xj} = Q^M_{xj} / n_j v_{Tj} T_j,$$

we obtain the thermodynamic forces-fluxes relation as

$$\begin{pmatrix} \widehat{\Gamma}^M_{xj} \\ \widehat{P}^M_{xj} \\ \widehat{Q}^M_{xj} \end{pmatrix} = -\frac{1}{\sqrt{\pi}} D_M \exp\left[-\frac{e\phi(x)}{\langle T \rangle}\right] \begin{pmatrix} K_0 & K_1 & K_3 \\ K_1 & K_2 & K_4 \\ K_3 & K_4 & K_5 \end{pmatrix} \begin{pmatrix} X_{1j} \\ X_{2j} \\ X_{3j} \end{pmatrix}. \tag{3.13}$$

The matrix elements K_0, K_1, K_2, K_3, K_4, K_5 are expressed as

$$K_0 = \frac{1}{\sqrt{\pi}} e^{-X_{0j}^2} + X_{0j}(1 - 2\Phi(\sqrt{2}X_{0j})),$$

$$K_1 = \Phi(\sqrt{2}X_{0j}) - \frac{1}{2},$$

$$K_2 = \frac{1}{\sqrt{\pi}} e^{-X_{0j}^2} + X_{0j}\left(\Phi(\sqrt{2}X_{0j}) - \frac{1}{2}\right),$$

$$K_3 = \frac{1}{\sqrt{\pi}} e^{-X_{0j}^2} + X_{0j}\left(\Phi(\sqrt{2}X_{0j}) - \frac{1}{2}\right),$$

$$K_4 = -\frac{1}{2\sqrt{\pi}} X_{0j} e^{-X_{0j}^2} + \frac{3}{2}\left(\Phi(\sqrt{2}X_{0j}) - \frac{1}{2}\right),$$

$$K_5 = \frac{1}{2\sqrt{\pi}} X_{0j}^2 e^{-X_{0j}^2} + \frac{2}{\sqrt{\pi}} e^{-X_{0j}^2} \frac{3}{2}\left(\Phi(\sqrt{2}X_{0j}) - \frac{1}{2}\right) X_{0j},$$

where $X_{0j} \equiv \dfrac{U_{/\!/ j}(x)}{v_{Tj}}$ and $\Phi(x)$ is the error function defined by

$$\Phi(x) = \frac{1}{\sqrt{2\pi}} \int_{-\infty}^{x} e^{-t^2/2} dt.$$

For the case where X_{0j} is small compared to unity, the error function is expanded with respect to X_{0j} and the terms up to the 2nd order of X_{0j} are retained. Noting that

$$\Phi(\mathrm{x}_{0j}) \simeq 1/2 - \frac{X_{0j}}{\sqrt{\pi}},$$

we obtain

$$\begin{pmatrix} \widehat{\Gamma}^M_{xj} \\ \widehat{P}^M_{xj} \\ \widehat{Q}^M_{xj} \end{pmatrix} = -\frac{1}{\pi} D_M \exp\left[-\frac{e\phi(x)}{\langle T \rangle}\right] \begin{pmatrix} 1+\frac{1}{2}X_{0j}^2 & X_{0j} & 1 \\ X_{0j} & 1 & X_{0j} \\ 1 & X_{0j} & 2 \end{pmatrix} \begin{pmatrix} X_{1j} \\ X_{2j} \\ X_{3j} \end{pmatrix}, \tag{3.13'}$$

where the determinant of the matrix up to the 2nd order of X_{0j} is given to be 1.

From Eq. (3. 13) (or Eq. (3. 13')) we see that another orthogonal relation between fluxes and forces can be chosen. However, here we adopt Eq. (3. 13') to consider the following transport process.

Ⅳ. Application of the Transport Matrix

Using the transport matrix (Eq. (3. 13')) obtained in the previous section, the formation of electric field and temperature distribution are examined.

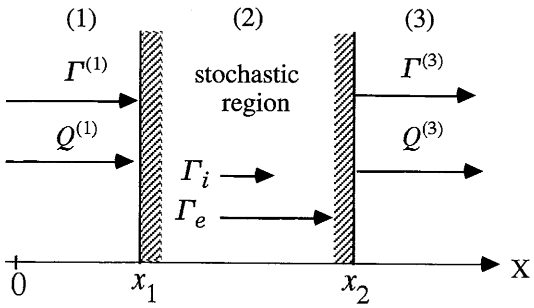

Fig. 10 The model plasma structure. The x axis is in the minor radius direction. The regions 1 and 3 are the magnetically non-stochastic region, and region 2 is the stochastic region. The particle flux and energy flux flow in the x direction.

IV-1. Electric Field Formation

Using the obtained matrix (Eq. (3. 13')), we study the generation of electric field in the stochastic region. In this region, the thermal velocity of electron is larger than that of ion, so that the electron flux is greater than the ion flux. The transport in this region is intrinsically bipolar and the electric field can be induced. The electric potential in the distribution function in Eq. (3. 2) is introduced so as to be consistent with this electric field.

We assume the model magnetic field structure, shown in Fig. (10), where the stochastic region is put between the non-stochastic regions. In the non-stochastic region, we assume that magnetic field lines form the magnetic surfaces. We label the non-stochastic region as 1, 3, and 2 for the stochastic region. We consider that the region 2 is thin and that the slab geometry can used.

In order to study the electric field formation in the stochastic region, the boundary conditions on the surface between regions 1 and 2as well as between region 2 and 3 are necessary. We consider a static case and impose the condition that the particle and heat fluxes across the boundaries are continuous. To this end the transport matrix in the non-stochastic region (1, 3 region) is assumed to be given as

$$\begin{pmatrix} \hat{\Gamma}_j^{(1,3)} \\ \hat{P}_j^{(1,3)} \\ \hat{Q}_j^{(1,3)} \end{pmatrix} = -\begin{pmatrix} \overline{D}_j & 0 & 0 \\ 0 & \overline{\mu}_j & 0 \\ 0 & 0 & \overline{\chi}_j \end{pmatrix} \begin{pmatrix} X_{1j}^{(1,3)} \\ X_{2j}^{(1,3)} \\ X_{3j}^{(1,3)} \end{pmatrix}, \tag{4.1}$$

where $\overline{D}_j$, $\overline{\mu}_j$ and $\overline{\chi}_j$ are the effective diffusivity, viscosity and heat conductivity, respectively. We, in this article, consider the case where the transport mechanisms in region 1 and in region 3 are the same and hence the same transport matrix can be used. The matrix in the stochastic region (region 2) is given by Eq. (3. 13'), and we assume that the mean particle velocity is small enough compared with the thermal velocity, that is $X_{0j} \simeq 0$. We use the superscripts (1, 3) and (2) for distinguishing the regions. The corresponding thermodynamic forces are

$$X_{1j}^{(k)} = \varkappa^{(k)} - \frac{1}{2}\varkappa_{Tj}^{(k)} \pm \frac{e}{\langle T \rangle} E^{(k)},$$

$$X_{3j}^{(k)} = \varkappa_{Tj}^{(k)},$$

$$\varkappa^{(k)} \equiv \frac{1}{n^{(k)}} \frac{dn^{(k)}}{dx},$$

$$\varkappa_{Tj}^{(k)} \equiv \frac{1}{T_j^{(k)}} \frac{dT_j^{(k)}}{dx},$$

where (k)=(1, 3) or (2).

The continuity conditions of the heat flux across the boundaries are given by

$$\hat{Q}_j^{(1)} = \hat{Q}_j^{(2)} = \hat{Q}_j^{(3)}. \tag{4.2}$$

Ion and electron particle fluxes are constrained by,

$$\Gamma_e^{(1)} = \Gamma_i^{(1)},\ \Gamma_e^{(2)} = \Gamma_i^{(2)},\ \Gamma_e^{(3)} = \Gamma_i^{(3)}, \tag{4.3}$$

which are the ambipolar conditions. And the continuity conditions are

$$\Gamma_e^{(1)} = \Gamma_e^{(2)} = \Gamma_e^{(3)}. \tag{4.4}$$

Imposing these conditions, we calculate the electric field in each region, which is obtained as

$$E^{(1,3)} = \frac{\langle T \rangle}{e(\overline{D}_i + \overline{D}_e)} \left[-\varkappa^{(1,3)}(\overline{D}_e - \overline{D}_i) + \frac{1}{2}(\overline{D}_e \varkappa_{Te}^{(1,3)} - \overline{D}_i \varkappa_{Ti}^{(1,3)}) \right], \tag{4.5-A}$$

$$E^{(2)} = -\frac{\langle T \rangle}{4ea} [\overline{\chi}_e \varkappa_{Te}^{(1,3)} - \overline{\chi}_i \varkappa_{Ti}^{(1,3)}], \tag{4.5-B}$$

$$a \equiv \frac{1}{\pi} D_M \exp\left[-\frac{e\phi(x)}{\langle T \rangle} \right].$$

For the convenience the electron diffusivity is taken as the same as the ion diffusivity in regions 1 and 3, that is $\overline{D}_e = \overline{D}_i$. Equation (4. 5-A) is rewritten as

$$E^{(1,3)} = \frac{\langle T \rangle}{4e} [(\varkappa_{Te}^{(1,3)} - \varkappa_{Ti}^{(1,3)}]. \tag{4.5-A'}$$

The electric field in region 2, $E^{(2)}$ should be consistent with the potential $\phi(x)$. Equation (4. 5-B) is rewritten as

$$\frac{d}{dx}\left\{ \exp\left[-\frac{e\phi(x)}{\langle T \rangle} \right] \right\} = \frac{\pi}{4D_M} \{\chi_e \varkappa_{Te}^{(1,3)} - \chi_i \varkappa_{Ti}^{(1,3)}\}$$

$$= \frac{\pi}{4D_M} \left\{ \frac{q_e}{v_{Te} T_e} - \frac{q_i}{v_{Ti} T_i} \right\}, \tag{4.5-B'}$$

and the derivative d/dx operates the quantity in region 2. Quantities q_e, q_i T_e and T_i are the boundary values. The general solution of the potential in the region 2 is obtained as

$$-\frac{e\phi(x)}{\langle T\rangle}=\ln\left[\frac{\pi}{4D_M}\left\{\frac{q_e}{v_{Te}T_e}-\frac{q_i}{v_{Ti}T_i}\right\}(x-x_1)+\exp\left\{-\frac{e\phi(x_1)}{\langle T\rangle}\right\}\right], \tag{4.6}$$

where $\phi(x_1)$ is the potential at $x=x_1$. The generated radial electric field is given by $-\partial\phi/\partial x$. We have the normalized electric field as

$$-\frac{e}{\langle T\rangle}\frac{d\phi(x)}{dx}=\frac{\frac{\pi}{4D_M}\left[\frac{q_e}{v_{Te}T_e}-\frac{q_i}{v_{Ti}T_i}\right]}{\frac{\pi}{4D_M}\left[\frac{q_e}{v_{Te}T_e}-\frac{q_i}{v_{Ti}T_i}\right](x-x_1)+\exp\left\{-\frac{e\phi(x_1)}{\langle T\rangle}\right\}}, \tag{4.6'}$$

This electric field has hyperbolic dependence on x. We can see from Eq. (4. 6') that the electric field in the stochastic region, region 2, depends on the difference of the thermal mobility ratio, $\frac{q_j}{D_M v_{Tj}T_j}$, between ion's and electron's heat fluxes in the adjoined non-stochastic regions.

Ⅳ-2. **Temperature distribution**

Next using the transport matrix, Eq. (3. 13'), and model magnetic field structure assumed in Fig. 10, we consider the temperature distribution in the stochastic region. We impose the stationary condition and assume that the heat fluxes are constant as

$$q_{0j}\equiv q_j^{(1)}(x)=q_j^{(2)}(x)=q_j^{(3)}(x),$$

where the $q_j^{(k)}(x)$ is the heat flux, and consider the case where $q_e \gg q_i$. The electron heat flux in the region 1, 3 is described by

$$q_e^{(1,3)}(x)=\overline{\chi_{0e}}\frac{d}{dx}T_e^{(1,3)}(x), \tag{4.7}$$

The electron heat flux in the stochastic region is described by

$$\frac{q_e^{(2)}(x)}{v_{Te}T_e^{(2)}(x)}=-\frac{D_M}{\pi}\exp\left[-\frac{e\phi(x)}{\langle T\rangle}\right]\left(\frac{3}{2}\frac{1}{T_e^{(2)}(x)}\frac{\partial T_e^{(2)}(x)}{\partial x}+\frac{e}{\langle T\rangle}\frac{d}{dx}\phi(x)\right), \tag{4.8}$$

where we approximate as $\varkappa^{(k)}\simeq 0$. Combining Eq. (4. 6) with Eqs. (4. 7) and (4. 8), we obtain the temperature distribution in each region as

$$\begin{aligned} T_e^{(1)}(x) &= -\frac{q_{0e}}{\chi_{0e}}x+T_{0e},\\ T_e^{(3)}(x) &= -\frac{q_{0e}}{\chi_{0e}}(x-x_2)+T_{2e}, \end{aligned} \tag{4.9}$$

$$T_e^{(2)}(x)=\left(\frac{\frac{\pi\sqrt{m_e}}{\sqrt{2}D_M}q_{0e}(x-x_1)+T_{1e}{}^{3/2}\exp\left\{-\frac{e\phi(x_1)}{\langle T\rangle}\right\}}{\frac{\pi}{4D_M}\left[\frac{q_{0e}}{v_{Te}T_{1e}}-\frac{q_{0i}}{v_{Ti}T_{1i}}\right](x-x_1)+\exp\left\{-\frac{e\phi(x_1)}{\langle T\rangle}\right\}}\right)^{2/3}, \tag{4.10}$$

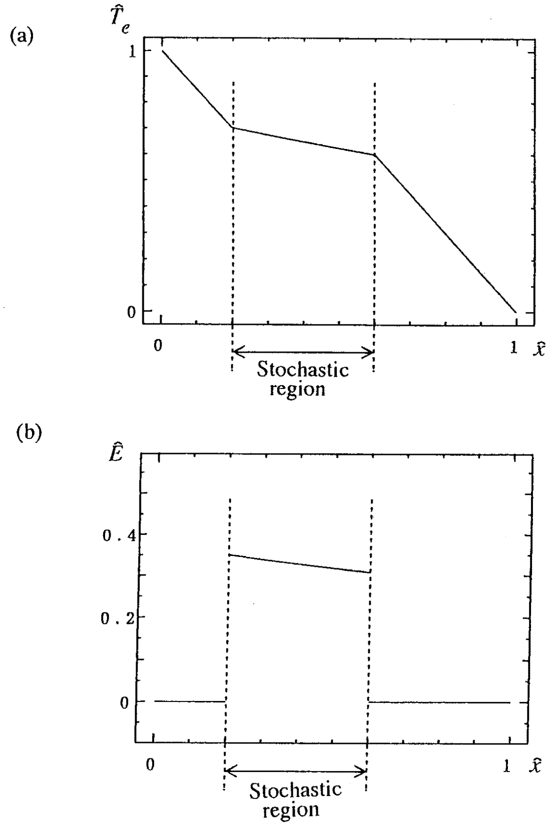

Fig. 11 (a) The resultant temperature distribution. (b) The induced electric field distribution. $\hat{T}_e$, $\hat{E}$ and $\hat{x}$ are the normalized temperature, normalized electric field and normalized minor radius. The stochastic region is bounded by $\hat{x}=0.2$ and $\hat{x}=0.6$.

where $\overline{\chi_{0e}}$ is chosen to be constant, $T_{0e}=T_e^{(1)}(0)$, $T_{1e}=T_e^{(1)}(x_1)$ and $T_{2e}=T_e^{(2)}(x_2)$.

Using Eqs. (4. 6), (4. 9) and (4. 10) we calculate the electric field and the temperature distribution for the parameters of a tokamak plasma, the major radius $R_0=3m$, the minor radius $a=1m$, $T_0=1keV$, $D_M=(\delta r)^2/2\pi R_0=5\times 10^{-5}m$, $\overline{\chi_{0e}}=10m^2/s$. Normalizations are given as $\hat{T}_e^{(k)}(x)=T_e^{(k)}(x)/T_{0e}$, $\hat{E}^{(2)}=E^{(2)}/(\langle T\rangle a/e)$ and $\hat{x}=x/a$. The results are shown in Fig. 3 for $q_{0e}=10keVm/s$, $q_{0i}=0keVm/s$. The temperature distribution in the stochastic region becomes flat and the positive radial electric field is formed in the stochastic region 2 (Fig. 11).

V. Summary and discussion

In summary we survey the dynamics of the magnetic field line which is used to describe the magnetic stochasticity, theoretical models of the anomalous particles diffusion and electron heat transport in the stochastic magnetic field lines and the experimental result of the temperature disruption in tokamak plasma are briefly discussed in Sec. II. In Sec. III we formulate the transport-matrix in a magnetically stochastic region from the kinetic equation. We take the moments the kinetic equation, where we assume that the distribution function is the shifted Maxwellian and includes the self-consistent electric potential. Then we obtain the plasma transport matrix (Ep. (3. 13)). We can see from the transport matrix, that the particle flow is induced by the temperature gradient as well as the density gradient, and heat flux is induced by the density gradient as well as temperature gradient.

By use of the obtained transport matrix, a simple study of the electric field generation and of the temperature distribution in this region are made in Sec. IV, where the model magnetic field has a layered structure in the radial direction. The electric field formation changes depending on the condition of heat flux in the non-stochastic region. The case for $q_e \gg q_i$ is considered. The electric field is generated due to the presence of stochastic magnetic diffusion and is formed in accordance with the heat conductivity and temperature gradient in the non-stochastic region. It has a hyperbolic dependence on x if D_M, $\bar{\chi}_e$ and $\bar{\chi}_i$ are uniformed. We also obtain the associated temperature distribution in the stochastic region. The temperature distribution in the stochastic region becomes flat and the positive radial electric field is formed in the stochastic region.

The generated electric field would induce the plasma motion. The flow is determined by the force from the electric field and the viscous drags in the stochastic/non-stochastic regions. Substituting the obtained electric field into the equation of motion as well as the heat transport equation (Eps. (3. 4) and (3. 5)), we may obtain the consistent electric field structure and the induced plasma flow. These are left for the future analysis.

On the other hand, the electric field as well as the associated dissipation affect the global MHD mode stability itself. The stability and the fluctuation level determine the characteristics of the stochasticity, e. g., the width of the region, the magnitude of D_M and whether the global stochasticity sets in or not, etc.. These effects are to be examined to obtain the consistent solution.

We only examined the one dimensional model. The MHD perturbations in tokamaks, including the magnetic island, have helical structures. The formation of the stochastic region is associated with the helical perturbation and is essentially two dimensional. In order to have deeper understanding of electric field formation, two dimensional model should be considered. This is left for our future work.

Acknowledgments

Author would like to express sincere thanks to Profs. K. Itoh, A. Fukuyama and A. J. Lichtenberg for fruitful discussions. The work is partly supported by Grant-in-Aid for Scientific Research of Ministry of Education, Science and Culture in Japan.

References

1) M. N. Rosenbluth, R. Z. Sagdeev, J. B. Taylor and G. M. Zaslavskij : Nucl. Fusion **6** (1966) 297.
2) T. H. Stix : Phys. Rev. Lett **30** (1973) 833.
3) A. B. Rechester and M. N. Rosenbluth : Phys. Rev. Lett. **40** (1978) 38.
4) T. H. Stix : Nucl. Fusion **18** (1978) 353.
5) B. B. Kadomtsev : Sov. J. Plasma Phys. **1** (1975) 389.
6) M. A. Dubois and A. Samain : Nucl. Fusion **20** (1980) 1101.
7) J. A. Krommes, C. Oberman and R. G. Kleva : J. Plasma Phys. **30** (1983) 11.
8) P. Kaw, E. J. Valeo and P. H. Rutherford : Phys. Rev. Lett. **43** (1979) 1398.
9) A. Boozer : J. Plasma Phys. **35** (1986) 133.
10) B. V. Waddel, B. Carreras, H. R. Hicks, J. A. Holmes and D. K. Lee : Phys. Rev. Lett. **41** (1978) 1386.
11) B. Carreras, H. R. Hicks, J. A. Holmes and B. V. Waddel : Phys. Fluids **23** (1980) 1811.
12) C. Mercier : Sov. J. Plasma Phys. **9** (1983) 82.
13) A. J. Lichtenberg : Nucl. Fusion **24** (1984) 1277.
14) A. J. Lichtenberg, K. Itoh, S.-I. Itoh and A. Fukuyama : Nucl. Fusion **32** (1992) 495.
15) D. J. Ward and S. C. Jardin : Nucl. Fusion **29** (1989) 905.
16) A. Y. Aydemir : Phys. Fluids **B2** (1990) 2135.
17) F. Porcelli : Phys. Fluids **30** (1987) 1734.
18) S. -I. Itoh and K. Itoh : Phys. Rev. Lett. **60**(1988) 2276 ; Papers from the 4th H-Mode Workshop (ed. by S. -I. Itoh) : Special Issue of Plasma Physics and Controlled Fusion **36** Suppl (7) A, (1994).
19) S. -I. Itoh : J. Phys. Soc. Jpn **59** (1990) 3431 ; K. Ida, S. -I. Itoh, K. Itoh et al. : Phys. Rev. Lett. **68** (1992) 182 ; K. Itoh, S. -I. Itoh, H. Sanuki and A. Fukuyama : IEEE Transactions on Plasma Science **22** (1994) 376.
20) A. J. Lichtenberg : Nucl. Fusion **24** (1984) 1277.
21) A. J. Lichtenberg, M. A. Lieberman : Regular and Stochastic Motion, Springer Verlag, New York (1984) Sect. 4. 2.
22) S. -I. Itoh, K. Itoh : Kakuyugo Kenkyuu, in Japan **67** (1992) 136.
23) A. B. Rechester and T. H. Stix : Phys. Rev. Lett. **36** (1976) 587.
24) G. M. Zaslavsky and B. V. Chirikov : Sov. Phys. Usp. **14** (1972) 549.
25) N. N. Filonenko, R. Z. Sagdeev and G. M. Zaslavsky : Nucl. Fusion **7** (1967) 253.
26) S. von Goeler, W. Stodiek and N. Sauthoff : Phys. Rev. Lett **33** (1974) 1201
27) D. J. Campbell, R. D. Gill, C. W. Gowers, J. A. Wesson, D. V. Bartlett, C. H. Best, S. Coda, A. E. Costley, A. Edwards, S. E. Kissel, R. M. Niestadt, H. W. Piekaar, R. Prentice, R. T. Ross, B. J. D. Tubbing : Nucl. Fusion **26** (1986) 1085.
28) V. V. Parail, G. V. Pereverzev : Sov. J. Plasma Phys. **6** (1980) 14.
29) W. Pfeiffer, Nucl. Fusion **25** (1985) 673.